Theoretical Study of Carbon Isotope Effects in the Nonclassical Carbonyl Cation CO/$[M(CO)_n]^+$ (M = Cu, Ag, Au; *n* = 1-4)

Yuriko Ono,[1,*] Takuro Tsutsumi,[2,3] Yu Harabuchi,[1,2] Tetsuya Taketsugu,[1,2,*]

Yasuhiko Fujii[4]

[1]*Institute for Chemical Reaction Design and Discovery (WPI-ICReDD), Hokkaido University, Sapporo 001-0021, Japan*

[2]*Department of Chemistry, Faculty of Science, Hokkaido University, Sapporo 060-0810, Japan*

[3]*L-Station, Creative Research Institution (CRI), Hokkaido University, Sapporo 060-0812, Japan*

[4]*Laboratory for Zero-Carbon Energy, Institute of Innovative Research, Tokyo Institute of Technology, 2-12-1 Ookayama Meguro Tokyo 152-8550, Japan*

Abstract:

In order to find an ideal exchange system for carbon isotope separation, carbon isotope effects in the CO/$[M(CO)_n]^+$ (M = Cu, Ag, Au; *n* = 1-4) complex system were analyzed using density functional theory calculations, and the isotopic equilibrium constants were calculated as the ratio of the reduced partition function ratios of the $^{13}C/^{12}C$ isotopic pairs. It is shown that the isotope equilibrium constant changes with the coordination number of CO to the complex as the temperature changes. In CO/$[Au(CO)_n]^+$, the contribution of bending vibration to the isotope effect increases, so that a higher isotope effect is expected than CO/$[Ag(CO)_n]^+$.

* Corresponding authors.

E-mail addresses: yono@icredd.hokudai.ac.jp (Y. Ono), take@sci.hokudai.ac.jp (T. Taketsugu).

1. Introduction

A group of noble metal carbonyl derivatives called "nonclassical metal carbonyls" has attracted much attention [1,2]. In metal carbonyls, the M-CO bond is usually formed by σ donation from CO to M and π backdonation from M to CO (classical carbonyl bond), and the CO bond becomes weaker by bonding with the metal. On the other hand, when M is a noble metal, π-backdonation does not occur efficiently due to the d^{10} electron configuration, so the CO bond becomes stronger with metal M (nonclassical carbonyl bond) because the CO HOMO (5σ) has an antibonding character with respect to C-O. Therefore, the C-O distance is shorter and the C-O stretching frequency is higher in nonclassical metal carbonyls than in free gas CO, resulting in a weaker and more unstable M-CO bond, which makes the CO ligand more reactive, and $M(CO)_n$ appears to have the properties of a high-performance catalyst. An application of $[Au(CO)_n]^+$ (n = 1, 2) as a catalyst was reported by Xu *et al.* [3].

The formation and nature of silver carbonyls in strong acids was reported by Souma *et al.* [4]. The coordination number of CO to Ag^+ in acid solvents decreases as the solvation tendency of the acid increases as H_2SO_4 > CF_3SO_3H > FSO_3H > HF, $BF_3 \cdot H_2O$. In H_2SO_4, $[Ag(CO)_2]^+$ has been reported to be formed at 20 atm of CO [5]. Furthermore, the formation of $Ag(CO)_2^+$ has been observed even under the atmospheric pressure of CO at 243 K [4]. $[Ag(CO)_2]^+$ is unstable and releases CO with increasing temperature, decomposing to Ag^+ and CO at 353 K. An experimental study by Xu [6] found that in concentrated H_2SO_4, only $[Ag(CO)]^+$ is formed. In HSO_3F, only $[Ag(CO)]^+$ is formed at room temperature, but at lower temperatures, $[Ag(CO)_2]^+$ is formed and reaches equilibrium with $[Ag(CO)]^+$. In magic acid $HSO_3F \cdot SbF_5$, a small amount of $[Ag(CO)_3]^+$ is formed when the temperature is lowered to 193 K. IR and Raman spectroscopy revealed

that $Ag(CO)_2^+$ has a linear structure [1]. Souma *et al.* reported the presence of $[Cu(CO)_n]^+$ (n = 3, 4) in the strong acid FSO_3H. It was found that $[Cu(CO)_3]^+$ and $[Cu(CO)_4]^+$ exist in equilibrium with $[Cu(CO)]^+$ as a mixture and that the equilibrium shifts with increasing temperature, decreasing CO pressure, and decreasing acid concentration. Du and Fujii [7] measured carbon isotope effects in the CO/$[Ag(CO)]^+$ system in FSO_3H + H_2SO_4 acid solvents in the temperature range 226-351 K at a pressure of 9.5×10^4 Pa and discussed the temperature dependence. In the low temperature region below 233 K, the carbon separation factors of the CO/$[Ag(CO)]^+$ complex system were observed to increase rapidly, and it was concluded that these increases were due to the formation of the $[Ag(CO)_2]^+$ complex.

Theoretical studies based on density functional theory (DFT) calculations have also been reported for the experimentally measured carbon isotope separation of isotope exchange reactions between metal carbonyls and CO [8,9]. In the analysis of the CO/$Ni(CO)_4$ system, a high correlation between experimental and calculated values was confirmed by appropriately considering the exchange reaction between $Ni(CO)_4$ and CO in the gas phase in addition to the gas-liquid CO exchange reaction [8]. In the analysis of the CO/$[Cu(CO)]^+$ system in ethanolamine, the temperature dependance was discussed by explicitly considering solvent effects [9].

In this study, we preform DFT calculations for $[Ag(CO)_n]^+$ (n = 1, 2) to elucidate the carbon isotope separation observed experimentally in the CO/$[Ag(CO)]^+$ complex system and to examine the effect of the number of ligands on the carbon isotope separation factor. We also apply these calculations to the CO/$[M(CO)_n]^+$ (M = Cu, Ag, Au; n = 1~4) system to further understand the carbon isotope effects in carbonyl complexes of these noble metals.

2. Theory

Quantum mechanical and statistical mechanical approaches can be used to treat isotope exchange reactions, just like other chemical reactions, on both macroscopic and molecular sizes [10-12]. For the isotope exchange reaction between A and B,

$$AX' + BX = AX + BX' , \quad (1)$$

the equilibrium constant K is represented as

$$\ln K = \ln\left(\frac{s}{s'}\right) f_{AX} - \ln\left(\frac{s}{s'}\right) f_{BX}, \quad (2)$$

where AX' is the lighter isotopomer, AX is the heavier isotopomer, A and B are two polyatomic molecular species attached by the lighter isotope X' or the heavier isotope X, s is the symmetry number, and $\ln(s/s')f_{AX}$ and $\ln(s/s')f_{BX}$ are the Bigeleisen-Mayer reduced partition function ratios (RPFRs) of the isotope pairs AX'/AX and BX'/BX, respectively. The partition function for molecular motion is calculated under the Born-Oppenheimer approximation, assuming that the potential energy surface is independent of isotopic substitution. It is also assumed that the total partition function is separable and factorizable into vibrational, rotational, translational, and other contributions, that the translational and rotational contributions at the temperature of interest can be considered classical and do not cause isotopic separation, and that vibrational motion is treated under the harmonic approximation.

The general formula for $(s/s')f$ is expressed as follows

$$\left(\frac{s}{s'}\right) f = \prod_{i=1}^{f_{vib}} \frac{u_i}{u_i'} \cdot \frac{\exp\left(-\frac{u_i}{2}\right)/\{1-\exp(-u_i)\}}{\exp\left(-\frac{u_i'}{2}\right)/\{1-\exp(-u_i')\}}. \quad (3)$$

Here, f_{vib} is the number of vibrational modes and u_i and u_i' are defined as

$$u_i = \frac{h\nu_i}{kT}, \; u_i' = \frac{h\nu_i'}{kT}. \quad (4)$$

where h is Planck's constant,ν_i and ν'_i are the frequencies of the ith vibrational mode of the molecular species containing heavy and light isotopes, respectively, k is Boltzmann's constant, and T is the absolute temperature. To discuss the isotope effects and their temperature dependence it is convenient to define a new function of the reduced energy, $b(u)$ [12]:

$$b(u) \equiv -\frac{1-e^{-u}}{ue^{-u/2}} \ , \tag{5}$$

then,

$$\ln\left(\frac{s}{s'}\right) f = \sum[\ln b(u'_i) - \ln b(u_i)], \tag{6}$$

Eqs. (2)~(6) show that the K-value of Eq. (1) can be theoretically calculated if all the vibrational frequencies of all the isotopic AX and BX species are known. The equilibrium constant K and the separation factor for the present system of CO *vs.* $[M(CO)_n]^+$ (M = Cu, Ag, Au; n = 1-4) are identical, because the symmetry numbers of ^{12}CO and ^{13}CO are unity, and those of the $[M(CO)_n]^+$ and their ^{12}C- and ^{13}C-isotopomers are all the same, so that the isotopic ratios of symmetry numbers cancel out [8,9].

3. Computational details

Geometry optimizations and normal mode analyses were performed for the complexes $[M(CO)_n]^+$ (M = Cu, Ag, Au; n = 1-4) in the solution of H_2SO_4, by the DFT method with the BP86 functional [13] and D3 version of Grimme's dispersion with Becke-Johnson damping [14], using the Gaussian16 program package [15]. The def2-QZVPP basis set [16], which is very computationally efficient and available for most atoms in the periodic table, was employed in the present calculations. The solvent effect of H_2SO_4 was incorporated by the Onsager model [17] where the dielectric constant of the solvent was set to 1.55, the value of sulfuric acid at 281.15 K [18]. The vibrational frequencies and normal mode vectors for isotopomers were calculated through the diagonalization of the mass-weighted Hessian matrices, taking into account with the appropriate atomic masses.

4. Results and discussion

In the previous report [7], the carbon isotope effect in the formation of Ag-CO complexes was studied using the following reaction,

$$[Ag(CO)_{n-1}]^+ + CO \leftrightarrow [Ag(CO)_n]^+. \quad (7)$$

The single-stage separation factor of an isotope exchange system is directly related to the equilibrium constant. The carbon isotope exchanges for the metal carbonyl can be written as,

$$[M(^{12}CO)_n]^+ + {}^{13}CO \leftrightarrow [M(^{12}CO)_{n-1}\,(^{13}CO)]^+ + {}^{12}CO \quad (8)$$

For the $^{13}C/^{12}C$, equilibrium constant K is given by the RPFR, Eqs. (2)~(6), as,

$$lnK = ln\left(\frac{s}{s'}\right) f\left[\left[M\left(^{13}CO\right)_{n-1}\left(^{12}CO\right)\right]^+ / [M\left(^{12}CO\right)_n]^+\right] - ln\left(\frac{s}{s'}\right) f[^{13}CO/^{12}CO] \quad (9)$$

In present study, DFT calculations were performed for nonclassical carbonyl cations, $[M(CO)_n]^+$ (M = Cu, Ag, Au; n = 1-4), which possess symmetric structures. The equilibrium geometry optimized with the solvent effect of H_2SO_4 are given in **Fig. 1**. Solvent effects on the structure were found to be very small.

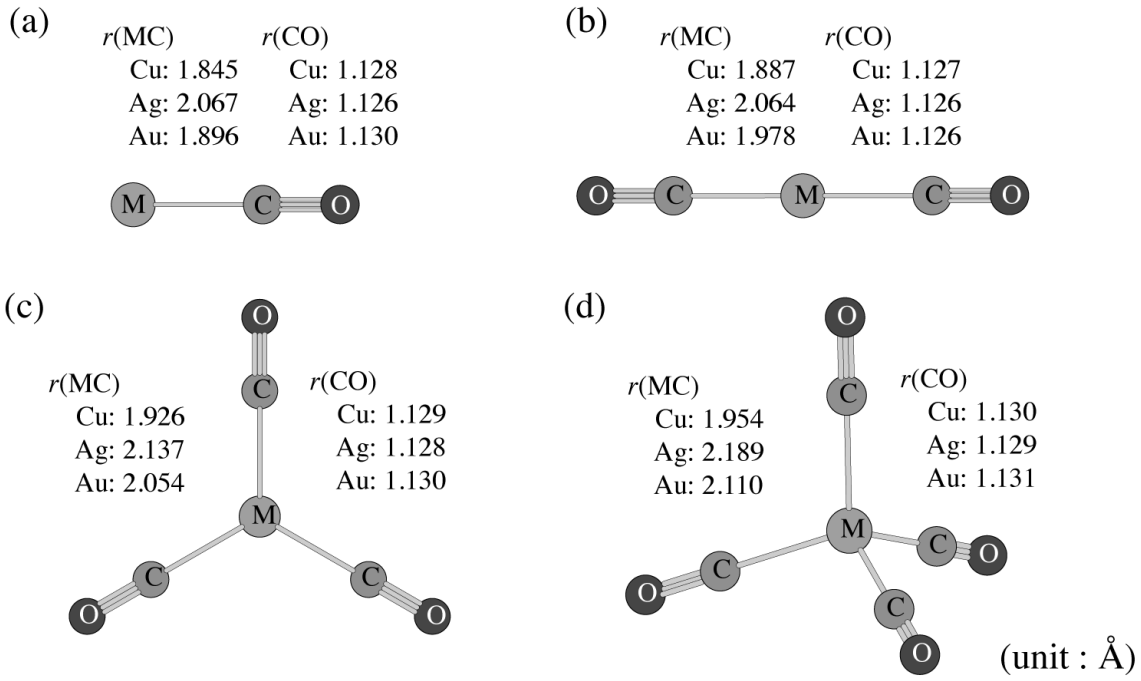

Fig. 1. The geometries of (a) $[M(CO)]^+$ in $C_{\infty v}$, (b) $[M(CO)_2]^+$ in $D_{\infty h}$, (c) $[M(CO)_3]^+$ in D_{3h}, and (d) $[M(CO)_4]^+$ in T_d point group, for M = Cu, Ag, and Au, optimized with the solvent effect of H_2SO_4. The bond lengths are given in Å.

The experimental value of the fundamental frequency of CO stretching vibration (ν(CO)) in the gas phase has been reported to be 2143 cm^{-1} [19], while the CO stretching fundamental frequencies of $[Ag(CO)^+]$ and $[Ag(CO)_2]^+$ determined by matrix isolation method were reported to be 2233.1 cm^{-1} and 2234.6 cm^{-1}, respectively [20]. This indicates that there is an electrostatic effect on the increase in ν(CO). If the molecule is placed in an electric field so that the carbon atom faces in the direction of increasing positive charge, the C-O bond becomes stronger and ν(CO) increases [21]. Whether the CO bond length of a carbonyl complex extends or contracts from the CO molecule is determined by the electrostatic interaction at the M-CO coordination bond and the σ-donation and π-backdonation between M and CO. Electrostatic M-CO interactions always favor CO

contraction, which becomes more pronounced as the effective nuclear charge of the transition metal increases [22].

An addition of a carbonyl ligand to $[Ag(CO)]^+$ increase the RPFR (and thus K). To understand this trend, the contributions from CO stretching vibrations of carbonyl to the RPFR of $[Ag(CO)_n]^+$ (n = 1, 2) at 263.15 K are listed in **Table 1**. Although the number of CO stretching vibration modes increases as the number of CO ligands increases, the isotopic shifts of the vibration modes decrease from 50.3 cm^{-1} (n = 1) to 41.8 cm^{-1} (CO antisym. str.) and 8.8 cm^{-1} (CO sym. str.) (n = 2), which means that the contribution from CO stretching vibration contribution from CO stretching vibrations changed only slightly from 1.1210 to 1.0997 × 1.0204 = 1.1221. However, the RPFR increased by 0.0046 at 263.15 K due to an increase in the contribution from angular displacement vibrations and stretching vibrations around carbon atoms.

Table 1. Analysis of the contributions to the RPFR of $[Ag(CO)_n]^+$ (n = 1, 2) and CO at 263.15 K obtained at the BP86+D3(BJ)/def2-QZVPP level of calculation. The solvent effect of H_2SO_4 was incorporated by the Onsager model [17]. The numbers in parentheses under each species represent the radius of the solute molecules used in Onsager-model calculations. The frequencies are given in cm^{-1}.

Species	Vibration Type	Frequencies $^{13}CO/^{12}CO$	$b(u)/b(u')$	RPFR (263.15K)	K
CO	CO str.	2075.1/2122.4	1.1127		
		overall		1.1127	
$[Ag(CO)]^+$	linear bend (×2)	220.1/226.8	1.0072		
(3.13 Å)	AgC str.	292.8/296.8	1.0028		
	CO str.	2153.6/2203.9	1.1210		
		overall		1.1323	1.0177
$[Ag(CO)_2]^+$	OC-Ag-CO bend (×2)	44.6/44.7	1.0000		
(3.43 Å)	AgCO bend (×2)	238.4/242.4	1.0046		
	AgCO bend (×2)	279.0/283.0	1.0054		
	AgC sym. str.	294.1/296.7	1.0019		
	AgC antisym. str.	321.1/322.7	1.0012		
	CO antisym. str.	2160.4/2202.2	1.0997		
	CO sym. str.	2215.3/2224.1	1.0204		
		overall		1.1369	1.0218

The weight given to the RPFR is the same for CO stretching modes alone, but the value of the RPFR is larger for $[Ag(CO)_2]^+$ due to the increase in the number of bending modes. In the experimental values reported for the CO/$[Ag(CO)_n]^+$ (n = 1, 2) system, K takes values between 1.0068 (at 303 K) and 1.0151 (at 233 K) [7]. The corresponding theoretical values are 1.0141-1.0214 for the CO/$[Ag(CO)]^+$ system and 1.0174-1.0265 for the CO/$[Ag(CO)_2]^+$ system, which are different from the experimental values. As mentioned previously, direct comparison of absolute values was difficult

because the isotope exchange system assumed was the simplest. Therefore, in this study, we decided to introduce an approximate formula by fitting a linear equation so that the calculated carbon isotope separation factors corresponds to the experimental values.

Figure 2 compares experimental and calculated carbon isotope separation factors for the CO/$[Ag(CO)_n]^+$ (n = 1, 2) system. The filled square indicates K_{exp} at 233.15 K, which corresponds to the CO/$[Ag(CO)_2]^+$ system, while the filled circles indicate K_{exp} at 263.15 K, 276.15 K, 288.15 K and 303.15 K, which correspond to the system CO/$[Ag(CO)]^+$. The concentration of CO absorbed in the 1.0 M Ag(I) solution system at a gas phase pressure of 9.5×10^4 Pa was observed experimentally. The CO concentration in the liquid phase exceeds the Ag^+ concentration, suggesting that the formation of $[Ag(CO)_2]^+$, represented by n = 2 in Eqs. (8) and (9), is not negligible in the low temperature region below 233 K. Then, a sharp increase in the carbon separation factor of the CO/Ag^I-CO complex system was observed in this temperature range. These increases may be due to the formation of $[Ag(CO)_2]^+$ complexes. On the other hand, the CO concentrations in solution at 263.15 K, 276.15 K, 288.15 K, and 303.15 K were below 1.0 M, suggesting that the K_{exp} corresponds to the CO/$[Ag(CO)]^+$ system.

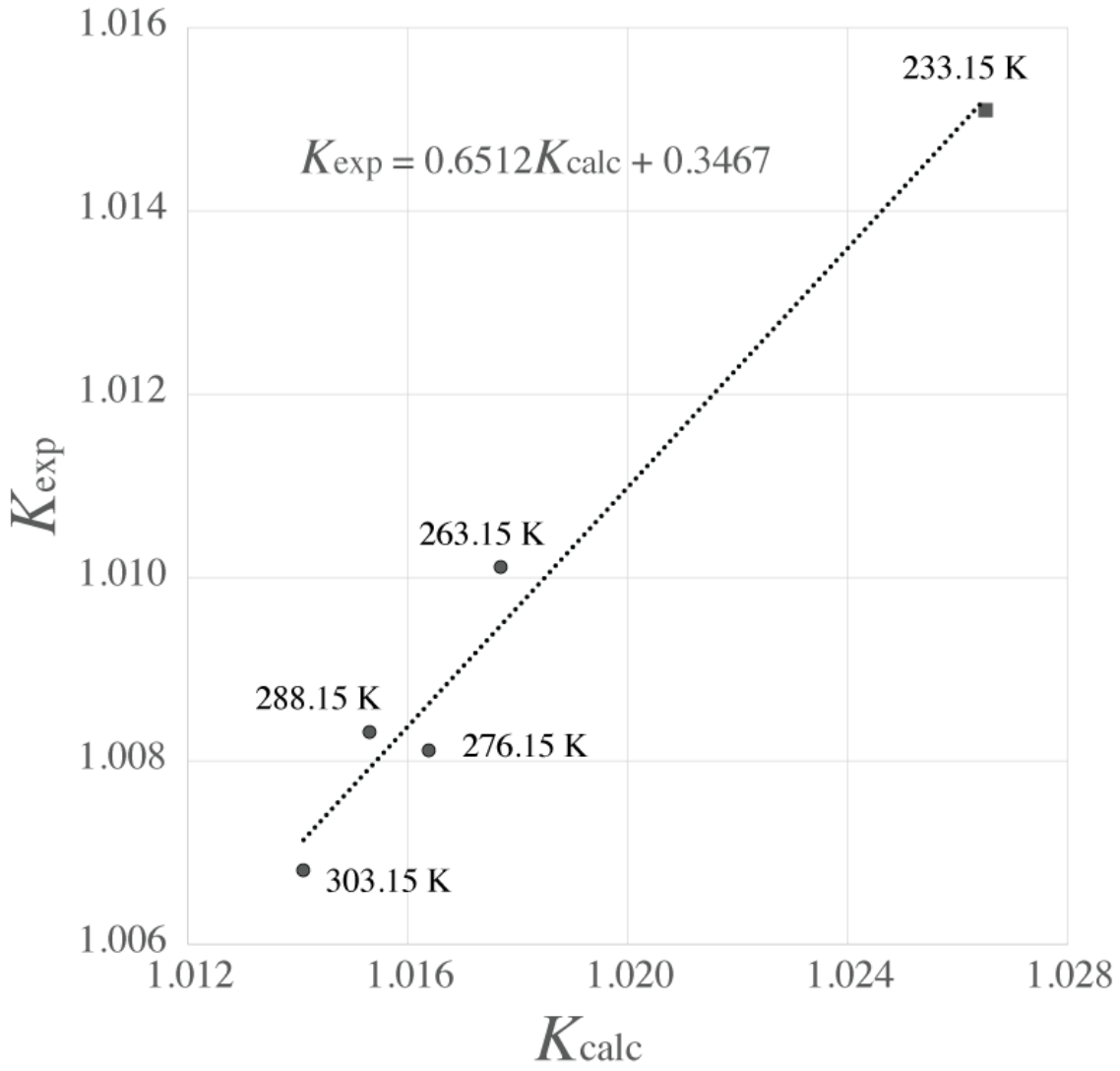

Fig. 2. The comparison between experimental and calculated carbon isotope separation factor for the system CO/$[Ag(CO)_n]^+$ (n = 1, 2). The filled square denote K_{exp} at 233.15 K, which corresponds to the system CO/$[Ag(CO)_2]^+$, while the filled circles denote K_{exp} at 263.15 K, 276.15 K, 288.15 K and 303.15 K, which corresponds to the system CO/$[Ag(CO)]^+$. An approximate formula for the relation of K_{calc} and K_{exp} obtained by fitting is also shown.

The temperature dependence of the carbon isotope effect in the CO/$[Ag(CO)_n]^+$ (n = 1, 2) system is plotted in **Fig. 3** based on the approximate formula obtained in Fig. 2. Filled square and filled circles indicate the experimental values for the CO/$[Ag(CO)]^+$ and CO/$[Ag(CO)_2]^+$ systems, respectively, while the theoretical values for the CO/$[Ag(CO)]^+$ and CO/$[Ag(CO)_2]^+$ systems are shown as solid lines and dashed lines, respectively. In the CO/$[Ag(CO)_n]^+$ system, a discontinuous increase in the carbon isotope effect was reported in the low-temperature region where CO adsorption exceeds 1.0 M. Theoretical calculations indicate that this phenomenon is due to the formation of $[Ag(CO)_2]^+$.

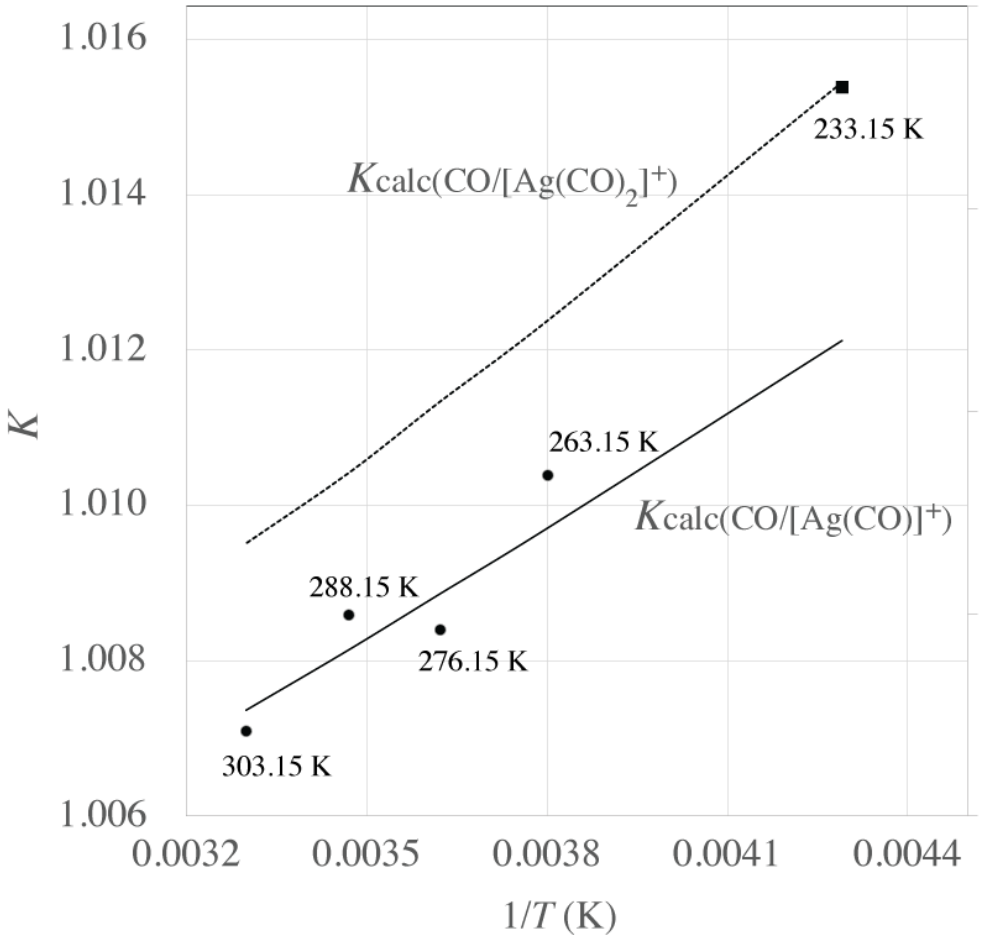

Fig. 3. The temperature dependence of carbon isotope effects in the $CO/[Ag(CO)_n]^+$ (n = 1, 2) system. Filled square and circles indicate experimental data, and the solid and dotted lines indicate the K_{calc} of $CO/[Ag(CO)]^+$ and $CO/[Ag(CO)_2]^+$, respectively. Notice that K_{calc} is corrected using the approximate formula between K_{exp} and K_{calc} shown in Fig. 2.

To further determine carbon isotope effects in carbonyl complexes of noble metals, calculations were also performed for the cupper and gold systems. **Table 2** shows the frequencies for $[M(CO)_n]^+$ (M = Cu, Au; n = 1, 2) with isotopic substitution from carbon mass 12 to 13, where the RPFR increases with the change from n = 1 to 2. Regarding the contribution of each frequency, in the case of $[Cu(CO)_2]^+$, the contribution of the CO stretching frequency to the RPFR is 1.0990 × 1.0298 = 1.1317, while in the case of $[Au(CO)_2]^+$, it is 1.0871 × 1.0340 = 1.1240. The reason why the RPFR is higher for $[Au(CO)_2]^+$ than for $[Cu(CO)_2]^+$ is due to the increased contribution of MCO-bending vibration.

Table 2. Analysis of the contributions to the RPFR of $[Cu(CO)_n]^+$ and $[Au(CO)_n]^+$ (n = 1, 2) and CO at 263.15 K obtained at the BP86+D3(BJ)/def2-QZVPP level of calculation. The solvent effect of H_2SO_4 was incorporated by the Onsager model [17]. The numbers in parentheses under each species represent the radius of the solute molecules used in Onsager-model calculations. The frequencies are given in cm^{-1}.

Species	Vibration Type	Frequencies $^{13}CO/^{12}CO$	$b(u)/b(u')$	RPFR (263.15K)	K
CO	CO str.	2075.1/2122.4	1.1127		
(2.87 Å)		overall		1.1127	
$[Cu(CO)]^+$	linear bend (×2)	279.2/287.8	1.0106		
(3.13 Å)	CuC str.	409.7/414.3	1.0044		
	CO str.	2148.4/2199.3	1.1228		
		overall		1.1409	1.0254
$[Cu(CO)_2]^+$	OC-Cu-CO bend (×2)	45.7/45.7	1.0000		
(3.54 Å)	CuCO bend (×2)	274.9/279.6	1.0062		
	CuCO bend (×2)	328.2/332.8	1.0072		
	CuC sym. str.	343.1/346.0	1.0024		
	CuC antisym. str.	398.3/400.0	1.0015		
	CO antisym. str.	2151.2/2189.1	1.0900		
	CO sym. str.	2213.6/2226.5	1.0298		
		overall		1.1421	1.0264
$[Au(CO)]^+$	linear bend(×2)	307.0/316.5	1.0142		
(3.03 Å)	AuC str.	432.5/438.7	1.0061		
	CO str.	2143.0/2194.6	1.1243		
		overall		1.1473	1.0311
$[Au(CO)_2]^+$	OC-Au-CO bend(×2)	58.8/58.8	1.0000		
(3.49 Å)	AuCO bend (×2)	297.7/302.5	1.0070		
	AuC sym. str.	354.1/356.6	1.0021		
	AuCO bend (×2)	397.6/404.0	1.0108		
	AuC antisym. str.	407.2/410.3	1.0030		
	CO antisym. str.	2153.9/2190.7	1.0871		
	CO sym. str.	2221.5/2236.2	1.0340		
		overall		1.1510	1.0345

RPFR analyses were also performed for $[M(CO)_n]^+$ (M = Cu, Au; n = 3, 4). Detailed results are shown in Table S1 in the Supplementary Material. **Figure 4** shows the correlation between the CO coordination number and the isotopic equilibrium constant for the CO/$[M(CO)_n]^+$ (M = Cu, Ag, Au; n = 1-4) system. As in the Ag system, the isotopic equilibrium constant decreases significantly as the CO coordination number increases. A similar increase is observed in the Cu series, but the increase is smaller than in the Ag series. The change from two to three-coordination decreases the isotopic equilibrium constants in all systems, but is particularly pronounced in the Au system. The formation of the gold(I) monocarbonyl cation, $[Au(CO)_n]^+$ (n = 1, 2), has been reported by Xu *et al.* [3]. Both $[Au(CO)]^+$ and $[Au(CO)_2]^+$ coexist in the concentrated H_2SO_4 solution, exhibiting IR absorptions at 2194 and 2208 cm^{-1} for n = 1 and n = 2, respectively. $[Au(CO)_3]^+$ and $[Au(CO)_4]^+$, which have low isotope equilibrium constants, are not formed even in FSO_3H solution. Therefore, the lower the temperature of the solution, the higher the equilibrium constant, which is advantageous for isotope separation. For CO/$[Au(CO)_2]^+$, the equilibrium constant (K_{calc}) is calculated to be 1.0345 at 263 K. This value is modified to 1.020 using the equation relating the experimental and theoretical values obtained in Fig. 2. This value is very large for a single-step isotope separation factor. On the other hand, $[Cu(CO)_3]^+$ and $[Cu(CO)_4]^+$ are known to form in FSO_3H solution. In the Cu system, the equilibrium constant increases as the coordination number increases from 1 to 2, but becomes smaller for 3- or 4-coordination complexes. Since 3- and 4-coordinated complexes have been experimentally confirmed in the Cu system, the solvent and adsorption amount should be carefully selected so that 2-coordination is predominant.

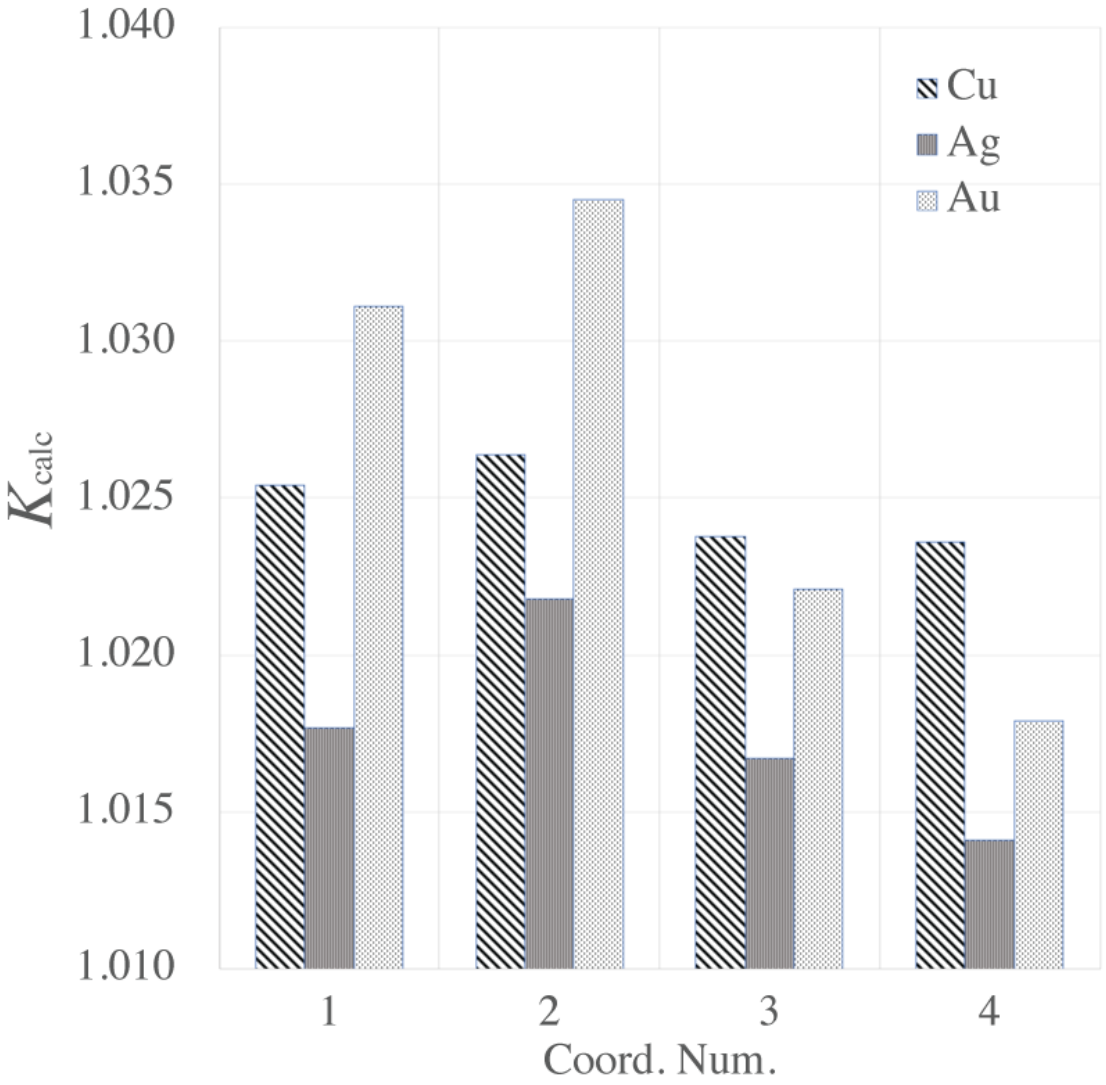

Fig. 4. The correlation between calculated isotopic equilibrium constants (K_{calc}) at 263 K and CO coordination number in the system CO/$[M(CO)_n]^+$ (M = Cu, Ag, Au; n = 1-4).

5. Conclusion

The carbon isotope effect in the CO /$[Ag(CO)_n]^+$ (n = 1, 2) complex system in H_2SO_4 solution was analyzed by DFT calculations using the Onsagare model and compared with experimental data. Our calculations reproduce the experimental report that the increase in CO adsorption on AgCl・FSO_3H solution at low temperatures is due to a change in the coordination number of CO, which significantly changes the carbon isotope effect. The calculations were also applied to the Cu and Au systems. In the CO/$[Au(CO)_n]^+$ complex system, as in the CO/$[Ag(CO)_n]^+$ complex system, the separation factor also increased as the coordination number increased from 1 to 2. The contribution of CO stretching to the isotope effect in the CO/$[Au(CO)_n]^+$ complex system is less than that in the CO/$[Ag(CO)_n]^+$ complex system, but the contribution of bending vibration to the isotope effect increases, so that a higher isotope effect is expected in total. In the low temperature region where $[Au(CO)_2]^+$ is formed in solution, a high carbon separation factor is expected.

Acknowledgments

We would like to dedicate this paper to the late Prof. Kozo Kuchitsu. Y. Ono is immensely grateful to the late Prof. Takanobu Ishida for his valuable supports and comments on an early stage of this study. T. Tsutsumi was financially supported by Wakeshima Makoto Research Fellowship. This work was partly supported by the Photo-excitonix Project in Hokkaido University, JST CREST Grant Number JPMJCR1902, and JSPS KAKENHI Grant Number JP22K14640. A part of calculations was performed using Research Center for Computational Science, Okazaki, Japan (Project: 22-IMS-C019).

References

[1] P. K. Hurlburt, J. J. Rack, J. S. Luck, S. F. Dec, J. D. Webb, O. P. Anderson, S. H. Strauss, Nonclassical Metal Carbonyls: $[Ag(CO)]^+$ and $[Ag(CO)_2]^+$, J. Am. Chem. Soc. 116 (1994) 10003–10014.

[2] G. Frenking, N. Fröhlich, The Nature of the Bonding in Transition-Metal Compounds, Chem. Rev. 100 (2000) 717–774.

[3] Q. Xu, Y. Imamura, M. Fujiwara, Y. Souma, A New Gold Catalyst: Formation of Gold(I) Carbonyl, $[Au(CO)_n]^+$ (n = 1, 2), in Sulfuric Acid and Its Application to Carbonylation of Olefins, J. Org. Chem. 62 (1997) 1594–1598.

[4] Y. Souma, J. Iyoda, H. Sano, Formation and Properties of Group 1B Metal Carbonyl Cations, Inorg. Chem. 15 (1976) 968–970.

[5] Y. Souma, H. Sano, THE ABSORPTION OF CARBON MONOXIDE BY SILVER-COMPOUNDS, Chem. Lett. (1973) 1059–1061.

[6] Q. Xu, Metal carbonyl cations: generation, characterization and catalytic application, Coord. Chem. Rev. 231 (2002) 83–108.

[7] J. Du, Y. Fujii, Temperature dependence of carbon isotope effects in CO/CO complex exchange reactions, Phys. Chem. Chem. Phys. 3 (2001) 5237–5241.

[8] Y. Ono, Y. Fujii, T. Ishida, A density functional theory study applied for carbon and oxygen isotope effects in the system $Ni(CO)_4$/CO, Chem. Phys. Lett. 390 (2004) 421–426.

[9] Y. Ono, Y. Fujii, S. Nagase, T. Ishida, A density functional theory study applied for carbon isotope effects in the non-aqueous $[Cu(CO)]^+$/CO system, Chem. Phys. Lett. 390 (2004) 71–78.

[10] J. Bigeleisen, Proceedings of International Symposium on Isotope Separation, J. Kistemaker, J. Bigeleisen, A. O. Nier, Eds., North Holland Publishing Co., Amsterdam (1958).

[11] T. Ishida, W. Spindel, J. Bigeleisen, Theoretical Analysis of Chemical Isotope Fractionation by Orthogonal Polynomial Methods, Isotope Effects in Chemical Processes, R. F. Gould, Ed., Advan. Chem. Series 89 (1969) 192–247.

[12] T. Ishida, Isotope Effect and Isotope Separation: A Chemist's View, J. Nuc. Sci. Tech. 39 (2002) 407–412.

[13] A. D. Becke, Density-functional exchange-energy approximation with correct asymptotic behavior. Phys. Rev A. 38 (1988) 3098–3100.

[14] H. Schröder, A. Creon, T. Schwabe, Reformulation of the D3(Becke–Johnson) Dispersion Correction without Resorting to Higher than C6 Dispersion Coefficients, J. Chem. Theory Comput. 11 (2015) 3163–3170.

[15] Gaussian 16, Revision C.01, M. J. Frisch, G. W. Trucks, H. B. Schlegel, G. E. Scuseria, M. A. Robb, J. R. Cheeseman, G. Scalmani, V. Barone, G. A. Petersson, H. Nakatsuji, X. Li, M. Caricato, A. V. Marenich, J. Bloino, B. G. Janesko, R. Gomperts, B. Mennucci, H. P. Hratchian, J. V. Ortiz, A. F. Izmaylov, J. L. Sonnenberg, D. Williams-Young, F. Ding, F. Lipparini, F. Egidi, J. Goings, B. Peng, A. Petrone, T. Henderson, D. Ranasinghe, V. G. Zakrzewski, J. Gao, N. Rega, G. Zheng, W. Liang, M. Hada, M. Ehara, K. Toyota, R. Fukuda, J. Hasegawa, M. Ishida, T. Nakajima, Y. Honda, O. Kitao, H. Nakai, T. Vreven, K. Throssell, J. A. Montgomery, Jr., J. E. Peralta, F. Ogliaro, M. J. Bearpark, J. J. Heyd, E. N. Brothers, K. N. Kudin, V. N. Staroverov, T. A. Keith, R. Kobayashi, J. Normand, K. Raghavachari, A. P. Rendell, J. C. Burant, S. S. Iyengar, J. Tomasi, M. Cossi, J. M. Millam, M. Klene, C. Adamo, R. Cammi, J. W. Ochterski, R. L. Martin, K. Morokuma, O. Farkas, J. B. Foresman, and D. J. Fox, Gaussian, Inc., Wallingford CT, 2016.

[16] F. Weigend, R. Ahlrichs, Balanced basis sets of split valence, triple zeta valence and quadruple zeta valence quality for H to Rn: Design and assessment of accuracy, Phys. Chem. Chem. Phys. 7 (2005) 3297–3305.

[17] M. W. Wong, M. J. Frisch, K. B. Wiberg, Solvent Effects 1. The Mediation of Electrostatic Effects by Solvents, J. Am. Chem. Soc. 113 (1991) 4776–4782.

[18] R. J. Gillespie, R. H. Core, The dielectric constant of sulphuric acid, Trans. Faraday Soc. 52 (1956) 1325–1331.

[19] K. P. Huber, G. Herzberg, Molecular Spectra and Molecular Structure, IV. Constants of Diatomic Molecules, Van Nostrand, New York, 1979.

[20] B. Liang, L. Andrews, Reactions of Laser-Ablated Ag and Au Atoms with Carbon Monoxide: Matrix Infrared Spectra and Density Functional Calculations on $Ag(CO)_n$ (n = 2, 3), $Au(CO)_n$ (n = 1, 2) and $M(CO)_n^+$ (n = 1-4; M = Ag, Au), J. Phys. Chem. A 104 (2000) 9156–9164.

[21] N. S. Hush, M. L. Wiliams, Carbon monoxide bond length, force constant and infrared intensity variations in strong electric fields: Valence-shell calculations, with applications to properties of adsorbed and complexed CO, J. Mol. Spectrosc. 50 (1974) 349–368.

[22] G. Bistoni, S. Rampino, N. Scafuri, G. Ciancaleoni, D. Zuccaccia, L. Belpassi, F. Tarantelli, How π back-donation quantitatively controls the CO stretching response in classical and non-classical metal carbonyl complexes, Chem. Sci. 7 (2016) 1174–1184.